Current Biology, Vol. 15, 935–941, May 24, 2005, ©2005 Elsevier Ltd All rights reserved. DOI 10.1016/j.cub.2005.04.059

# Functional Genomics of the Cilium, a Sensory Organelle

**Oliver E. Blacque,[1] Elliot A. Perens,[2] Keith A. Boroevich,[1] Peter N. Inglis,[1] Chunmei Li,[1] Adam Warner,[3] Jaswinder Khattra,[3] Rob A. Holt,[3] Guangshuo Ou,[4] Allan K. Mah,[1] Sheldon J. McKay,[3] Peter Huang,[3] Peter Swoboda,[5] Steve J.M. Jones,[3] Marco A. Marra,[3] David L. Baillie,[1] Donald G. Moerman,[6] Shai Shaham,[2] and Michel R. Leroux[1,*]**

[1]Department of Molecular Biology and Biochemistry
Simon Fraser University
8888 University Drive
Burnaby, British Columbia V5A 1S6
Canada

[2]Laboratory of Developmental Genetics
The Rockefeller University
1230 York Avenue
New York, New York 10021

[3]Genome Sciences Centre
British Columbia Cancer Agency
Vancouver, British Columbia V5Z 4E6
Canada

[4]Section of Molecular and Cellular Biology
Center for Genetics and Development
University of California, Davis
Davis, California 95616

[5]Department of Biosciences
Section of Natural Sciences
Karolinska Institute
Södertörn University College
S-14189 Huddinge
Sweden

[6]Department of Zoology
University of British Columbia
Vancouver, British Columbia V6T 1Z4
Canada

## Summary

**Cilia and flagella play important roles in many physiological processes, including cell and fluid movement, sensory perception, and development [1]. The biogenesis and maintenance of cilia depend on intraflagellar transport (IFT), a motility process that operates bidirectionally along the ciliary axoneme [1, 2]. Disruption in IFT and cilia function causes several human disorders, including polycystic kidneys, retinal dystrophy, neurosensory impairment, and Bardet-Biedl syndrome (BBS) [3–5]. To uncover new ciliary components, including IFT proteins, we compared *C. elegans* ciliated neuronal and nonciliated cells through serial analysis of gene expression (SAGE) and screened for genes potentially regulated by the ciliogenic transcription factor, DAF-19 [6]. Using these complementary approaches, we identified numerous candidate ciliary genes and confirmed the ciliated-cell-specific expression of 14 novel genes. One of these, C27H5.7a, encodes a ciliary protein that undergoes IFT. As with other IFT proteins, its ciliary localization and transport is disrupted by mutations in IFT and *bbs* genes. Furthermore, we demonstrate that the ciliary structural defect of *C. elegans dyf-13(mn396)* mutants is caused by a mutation in C27H5.7a. Together, our findings help define a ciliary transcriptome and suggest that DYF-13, an evolutionarily conserved protein, is a novel core IFT component required for cilia function.**

## Results and Discussion

### Identification of Candidate Ciliary Genes through SAGE and a Bioinformatic Screen for Genes Potentially Regulated by X Box Promoter Elements

In the first approach, we used LongSAGE to obtain a *C. elegans* ciliated-cell transcriptome. Ciliated neurons expressing GFP from the ciliated-cell-specific *bbs-1* gene promoter [5] were isolated and used to construct a LongSAGE library as described [7, 8]. To identify candidate ciliary genes, we compared our ciliated-cell SAGE transcriptome to pan-neural-, muscle-, and gut-specific transcriptomes, all normalized to 50,000 tags (available at http://www.bcgsc.ca). Because ciliated neurons account for only ~20% of all embryonic neurons, genes expressed predominantly in ciliated neurons should be represented by more SAGE tags in the ciliated-cell (C) transcriptome than in the pan-neural (P) transcriptome. Similarly, ciliated-cell-specific transcripts should be underrepresented in the nonciliated muscle (M) and gut (G) transcriptomes. Table S1 (in the Supplemental Data available with this article online) presents the SAGE data, sorted by genes with the most favorable ciliated-cell SAGE tag enrichment factors across all three comparison groups (C/P, C/M, and C/G). As expected, the top-ranked genes from Table S1 contain numerous cilia-related genes, including IFT-related genes (*daf-19*, *bbs-1*, *che-2*, *che-13*, and *osm-6*), structural components (*tba-9*, *tba-6*, and *mec-12)* and motor components (F41G4.1, axonemal dynein; *dli-1*, cytoplasmic dynein; and *klp-11*, kinesin). To assess the specificity of our SAGE approach in detecting ciliated-cell-specific genes, we screened Table S1 for genes known to be expressed predominantly in ciliated cells; 25 of 42 such genes found (60%) were enriched for SAGE tags in the ciliated-cell transcriptome versus the pan-neural, muscle, and gut transcriptomes (Table S2). These data suggest that Table S1 likely contains many excellent candidate ciliary genes. To estimate the proportion of false positives in Table S1, we investigated the top 200 genes and found 51 genes with known expression data; 34 of these genes (67%) are expressed in nonciliated cells, indicating a relatively high but acceptable false-positive rate. On the basis of these findings, we sought to further refine our search for can-

*Correspondence: leroux@sfu.ca

didate cilia-related genes with a complementary approach.

We performed a genome-wide bioinformatic screen for genes potentially regulated by X boxes. In *C. elegans*, these conserved 14 bp regulatory elements (usually 50–150 bp upstream of start codons) are bound by DAF-19, the RFX-type transcription factor that regulates ciliary gene (IFT and *bbs*) expression [5, 6, 9, 10]. We derived an improved X box consensus sequence for our screen by confirming the ciliated-cell-specific expression of several candidate X-box-containing genes identified in a previous, more preliminary study [9]. Using transcriptional-GFP reporters, we observed ciliated-cell-specific expression for five novel genes, namely K03E6.4, C48B6.8, C47E8.6, ZK328.7a, and F19H8.3 (Figure S1; data not shown for F19H8.3). Figure S1 also shows the ciliated-cell-specific pattern for Y110A7A.20 and K08D12.2, which were not shown in our previous study [9]. Importantly, the expression of ZK328.7a, Y110A7A.20, and C48B6.8 was found to be dependent on DAF-19 (Figure S2). Using an updated Hidden Markov Model X box profile based on 22 sequences, including the novel X-box-containing genes discussed above (Table S3), we scanned the *C. elegans* genome for X boxes within 1500 bp upstream of start codons. A total of 1572 putative X-box-containing genes with human homologs were identified (Table S4). As expected, the greatest number of high-scoring (>16.0) X boxes occurred between −60 and −120 bp (Figure S3A), which coincides with the canonical position [6].

As described above for the SAGE data, we found that the number of false positives in Table S4 is relatively high, but the dataset still contains a large proportion of bona fide ciliary genes. Of the top 200 ranked candidate X box genes with known anatomic expression data (64 genes), 27 (or 42%) are expressed in ciliated cells.

To identify our best candidate ciliary genes, we considered genes with enrichment of SAGE tags in the ciliated SAGE dataset versus the pan-neural, muscle, and intestine datasets (Table S1), *and* with putative X boxes within 250 bp of start codons (Table S4). Using these criteria, we present 46 such genes in Table 1. Also included are seven additional genes (at the bottom of Table 1), which rank highly in *either* the SAGE *or* X box datasets. As expected, Table 1 contains many known IFT-related genes, including *che-2*, *che-13*, *osm-1*, *osm-5*, *osm-6*, F32A6.2 (IFT81), *bbs* genes, and *daf-19*. Other excellent candidate and known ciliary genes include K08D12.2 (homolog of retinitis pigmentosa 2), which is expressed predominantly in ciliated neurons (Figure S1), and Y32G9A.6, an ankyrin-repeat-containing protein that is homologous to inversin, which is linked to cilia-associated *situs inversus* and cystic-kidney phenotypes [11]. Table 1 also includes uncharacterized genes identified as candidate ciliary genes in other genomic and proteomic screens [10, 12, 13]; these genes include C27H5.7a (TPR containing), C54G7.4 (WD repeat containing), K07G5.3 ($Ca^{2+}$ binding domain containing), and two B9-protein-domain-containing genes (Y38F2AL.2 and K03E6.4), as well as several genes not previously associated with a ciliary function. C27H5.7a is particularly interesting because it was also recently found by Colosimi et al. [14] to be expressed in the AWB ciliated olfactory neuron. Importantly, the number of false-positive genes in Table 1 is relatively low; 13 of the 20 genes from Table 1 with known anatomic expression data (WormBase [http://www.wormbase.org] and Figure S1) are expressed in ciliated cells. Along with GFP-expression data presented below, we estimate the false-positive rate for the top 46 genes in Table 1 to be approximately 26% (7 of 27 genes), which is significantly lower than that found for the individual SAGE (67%) and X box (58%) analyses.

### Expression Analysis of Candidate Ciliated-Cell-Specific Genes

Nine new candidate ciliated-cell-specific genes were chosen for expression analysis on the basis of strong SAGE *and* X box data (Table 1; seven genes) or a high ranking in the individual X box table (Table S4; two genes). Using transgenic worms bearing promoter-GFP reporters, we found that all nine genes demonstrated a ciliated-cell-specific expression pattern (Figure 1; data not shown for C02H7.1). Transcriptional *gfp* reporters for C27H5.7a (unknown function), Y38F2AL.2 (B9 domain containing), H01G02.2 (serine/threonine kinase), C54G7.4 (WD domain containing), D1009.5 (dynein light chain), and Y32G9A.6 (inversin-like) produced strong GFP signals in most ciliated cells, including amphid, phasmid, and labial-quadrant neurons. Similarly, F54C1.5a (TPR domain containing) and K07G5.3 ($Ca^{2+}$ binding domain containing) expressed in most amphid, both phasmid, and several labial-quadrant neurons. That the expression of the *gfp* reporters was not detected in nonciliated cells suggests that these novel genes have ciliary functions. It is notable that all of the genes selected from Table 1 for expression analysis demonstrated a ciliated-cell expression pattern. This is a very strong indication that Table 1 is highly enriched for novel cilia-related genes.

### Cellular Localization of Candidate Ciliary Proteins

To investigate the possible functions of some of the ciliated-cell-specific proteins identified above, namely C27H5.7a, Y37E3.5, K08D12.2, and F19H8.3, we examined their cellular localization with translational *gfp* reporters (Figure S4A). Interestingly, GFP-tagged C27H5.7a (unknown function) and Y37E3.5 (GTP binding protein, ARL2-like-1) associate with ciliary axonemes in both head (amphids, labials) and tail (phasmids) neurons, with relatively little localization to cell bodies, axons, or dendrites. In addition, C27H5.7a::GFP localizes to the transition zones (basal bodies at the base of cilia). GFP-tagged Retinitis Pigmentosa 2 homolog K02D12.2 appears to envelop the transition zones in a ring-like fashion (Figure S4A), indicating a possible role at the base of cilia. GFP-tagged ARL-3 (F19H8.3) is found throughout the cell, with little ciliary localization even though its expression is limited to ciliated cells.

### C27H5.7a Is a Novel IFT-Associated Protein

A major focus of our functional genomic studies is to uncover novel core ciliary proteins, including IFT com-

Table 1. SAGE and X Box Data Identify a Set of Strong Candidate Cilia-Related Genes

| Gene | | SAGE Data | | | | Xbox Data | | | Other Studies | | | | Annotation / |
|---|---|---|---|---|---|---|---|---|---|---|---|---|---|
| Model | Name | C | P | M | G | Sequence | Pos. | Score | A | B | C | D | Description |
| Y105E8A.5 | *bbs-1* | 19 | 1 | 0 | 0 | GTTCCCATAGCAAC | 98 | 19.29 | ✓ | ✓ | | | BBS1 |
| F59C6.7 | *che-13* | 26 | 3 | 1 | 1 | GTTGCTATAGCAAC | 73 | 17.70 | ✓ | ✓ | ✓ | | IFT57 |
| C27H5.7a | | 8 | 0 | 0 | 1 | GTCTCCATAGCAAC | 102 | 19.07 | ✓ | ✓ | ✓ | ✓ | Uncharacterized |
| T06G6.3 | | 7 | 1 | 0 | 0 | GTTGCCATGGCAAA | 59 | 16.11 | | | | | Myosin heavy chain-like |
| Y38F2AL.2 | | 6 | 1 | 0 | 0 | GTTGCCGTGGCAAC | 65 | 16.11 | ✓ | ✓ | | | B9 domain containing |
| R31.3 | *osm-6* | 6 | 1 | 0 | 0 | GTTACCATAGTAAC | 99 | 18.68 | ✓ | ✓ | | | IFT52 |
| F32A6.2 | | 5 | 1 | 0 | 0 | GTTGCCCTGGTAAC | 71 | 16.85 | ✓ | | ✓ | | IFT81 |
| F38G1.1 | *che-2* | 5 | 1 | 1 | 1 | GTTGTCATGGTGAC | 129 | 16.30 | ✓ | ✓ | ✓ | | IFT80 |
| R13G10.2 | *amx-1* | 5 | 1 | 0 | 1 | GCTACCATGACAAC | 144 | 14.52 | | | | | Monoamine oxidase |
| F35D2.4 | | 5 | 1 | 0 | 0 | ATCACCATGACAAC | 158 | 12.85 | | | | | Uncharacterized |
| M04G12.3 | *gcy-34* | 4 | 0 | 1 | 0 | GTCTTCACAGCAAC | 122 | 11.09 | | ✓ | | | Guanylate cyclase |
| K10G6.4 | | 4 | 1 | 0 | 0 | GTCACCATGCCAAT | 139 | 12.85 | | | | | Uncharacterized |
| Y41G9A.1 | *osm-5* | 8 | 2 | 1 | 0 | GTTACTATGGCAAC | 114 | 19.79 | ✓ | ✓ | ✓ | | IFT88 |
| W02B12.3c | *rsp-1* | 7 | 0 | 2 | 1 | GTTGTCATGGCTAC | 131 | 15.18 | | | | | Splicing factor |
| F33H1.1b | *daf-19* | 28 | 8 | 6 | 7 | GTTTCCATGGAAAC | 108 | 19.61 | | | | | RFX transcription factor |
| F08C6.4 | *sto-1* | 30 | 9 | 8 | 6 | TTTTCCTTGGTAAC | 201 | 12.69 | | | | | Stomatin |
| K03E6.4 | | 3 | 1 | 0 | 0 | GTTCCCTTGGCAAC | 83 | 17.11 | ✓ | | | | B9 domain containing |
| F13B9.5 | *ksr-1* | 3 | 1 | 1 | 0 | TTTTTCTTGGCAAC | 104 | 10.65 | | | | | Kinase regulator of Ras |
| Y32G9A.6 | | 3 | 1 | 0 | 0 | GTTGTCAGGGTAAC | 186 | 13.52 | | | | | Inversin-like |
| Y41D4A.4 | | 6 | 1 | 0 | 2 | GTTGCCACGTTAAC | 140 | 12.46 | | | | | EMP70 |
| F32A6.5 | *sto-2* | 6 | 1 | 2 | 1 | GTTTCCTTAAAAAC | 181 | 11.48 | | | | | Stomatin |
| F28E10.1c | | 11 | 4 | 0 | 2 | GTCGCCAGAGCAAC | 80 | 13.09 | | | | | Titin/Connectin |
| F20D12.3 | *bbs-2* | 8 | 3 | 0 | 1 | GTATCCATGGCAAC | 93 | 20.02 | ✓ | | | | BBS2 |
| ZC84.6 | | 5 | 2 | 1 | 0 | GTTTATTTGGTAAC | 99 | 11.11 | | | | | Serine protease inhibitor |
| Y37A1A.3 | | 2 | 0 | 0 | 0 | GTCAATATGACAAC | 178 | 10.26 | | | | | Glucose transporter |
| B0228.5a | | 2 | 1 | 0 | 1 | GTTACCATATCAGC | 16 | 11.18 | | | | | Thioredoxin |
| B0432.5a | *cat-2* | 2 | 1 | 0 | 0 | GTCCCCACGCCAAC | 36 | 10.97 | | ✓ | | | Tyrosine hydroxylase |
| F56H11.1c | *fbl-1* | 2 | 1 | 1 | 0 | GTTTCCGTTACAAC | 76 | 10.09 | | ✓ | | | Fibulin |
| K08D12.2 | | 2 | 1 | 0 | 0 | GTTTCCATAGCAAC | 83 | 20.74 | ✓ | | | | Retinitis pigmentosa 2 |
| C27F2.1 | | 2 | 1 | 1 | 0 | GTCACCATAGCAAC | 83 | 18.41 | | | | | Uncharacterized |
| T27B1.1 | *osm-1* | 2 | 0 | 0 | 1 | GCTACCATGGCAAC | 85 | 17.91 | ✓ | ✓ | ✓ | | IFT172 |
| C09E10.2b | *dgk-1* | 2 | 1 | 0 | 0 | GTACTCATGCTAAC | 131 | 10.30 | | | | | Diacylglycerol kinase |
| H01G02.2 | | 2 | 1 | 1 | 0 | GTCTCCATGACAAC | 159 | 16.96 | | | | | Serine/Threonine kinase |
| C26B9.5 | | 2 | 0 | 0 | 1 | GTTTGCATAGTCAC | 174 | 10.41 | | | | | Serine protease |
| T01D1.6 | *abu-11* | 2 | 0 | 0 | 0 | GTCAACATAACAAC | 229 | 10.56 | | | | | Keratin associated |
| K07G5.3 | | 6 | 3 | 1 | 1 | GTTGCCATAGCGAC | 70 | 17.30 | | ✓ | | | Uncharacterized |
| K06H7.3 | | 6 | 3 | 1 | 1 | TTTTCCATAATAAC | 238 | 11.48 | | | | | Ankyrin repeat protein |
| R166.3 | | 6 | 3 | 2 | 3 | ATCTCCTTGGCAAC | 248 | 13.43 | | | | | AMME Syndrome 1 |
| R11A8.2 | | 7 | 4 | 0 | 0 | GTTTCCATATTAAT | 225 | 11.48 | | | | | G patch and KOW motifs |
| ZK1151.1c | *vab-10* | 7 | 4 | 1 | 0 | GTTTTTATGGCAAA | 235 | 12.52 | | | | | MACF1 |
| R01H10.6 | *bbs-5* | 19 | 11 | 2 | 3 | GTCTCCATGGCAAC | 64 | 20.35 | ✓ | ✓ | | | BBS5 |
| T24D1.1b | *sqv-5* | 5 | 3 | 0 | 0 | GTTCCTTCGGCAAC | 33 | 11.00 | | | | | Chodroitin synthase 2 |
| F59D12.1 | | 3 | 2 | 1 | 0 | ATTACCATAGTTAC | 170 | 12.92 | | | | | Transmembrane protein |
| C02H7.1 | | 3 | 2 | 0 | 0 | GTCTCCATGACAAC | 194 | 16.96 | ✓ | ✓ | | | Uncharacterized |
| D1009.5 | | 6 | 4 | 2 | 2 | GTTGCCATGACAAC | 76 | 17.18 | ✓ | ✓ | | | Dynein light chain |
| C48B6.8 | | 6 | 4 | 2 | 0 | GTTTCCATGACAAC | 80 | 18.63 | | | | | B1 protein |
| F08B12.1 | | 13 | 1 | 1 | 1 | | | | | | | | Prominin 1 |
| ZK520.1 | | 8 | 2 | 1 | 2 | | | | ✓ | ✓ | | | WD-repeat domain 19 |
| C54G7.4 | | 4 | 4 | 0 | 0 | GTTGCCATGGCAAT | 172 | 17.11 | ✓ | ✓ | | | WD-repeat protein 35 |
| F54C1.5a | | 3 | 3 | 1 | 2 | GTTACCATGGATAT | 105 | 15.50 | ✓ | ✓ | | | TPR repeat containing |
| ZK328.7a | | 1 | 1 | 1 | 0 | GTTACCATGGCAAT | 88 | 17.91 | ✓ | | | | TPR repeat containing |
| F19H8.3 | | 1 | 6 | 2 | 1 | GTCTCTATGGTAAC | 150 | 17.35 | | ✓ | | | ARL3 |
| C47E8.6 | | 0 | 0 | 0 | 0 | GTTACCATGCCAAC | 108 | 17.98 | | | | | Uncharacterized |

Shown are all genes (46 in total) that are enriched for SAGE tags in the ciliated-cell transcriptome (C), with $\geq$1.5-fold enrichment versus the pan-neural transcriptome (P) and $\geq$2.0-fold enrichment versus the muscle (M) and gut (G) transcriptomes, *and* with a canonically-positioned (Pos) putative X box (i.e., within 250 bp of the start codon). Only genes with homology to a human gene (Blast E-value < $e^{-10}$) are represented. Genes are sorted according to the level of SAGE tag enrichment in the ciliated-cell transcriptome versus the other three transcriptomes. The seven candidate cilia-related genes at the bottom of the table are included on the basis of their high ranking in the individual SAGE *or* X box tables (Tables S1 and S4, respectively). Check marks indicate genes identified as candidate ciliary genes in three previous genomics and proteomics studies, namely (A) Li et al. [10], (B) Avidor-Reiss et al. [12], and (C) Ostrowski et al. [13], or as a sensory-neuron-type-specific gene ([D] Colosimo et al. [14]).

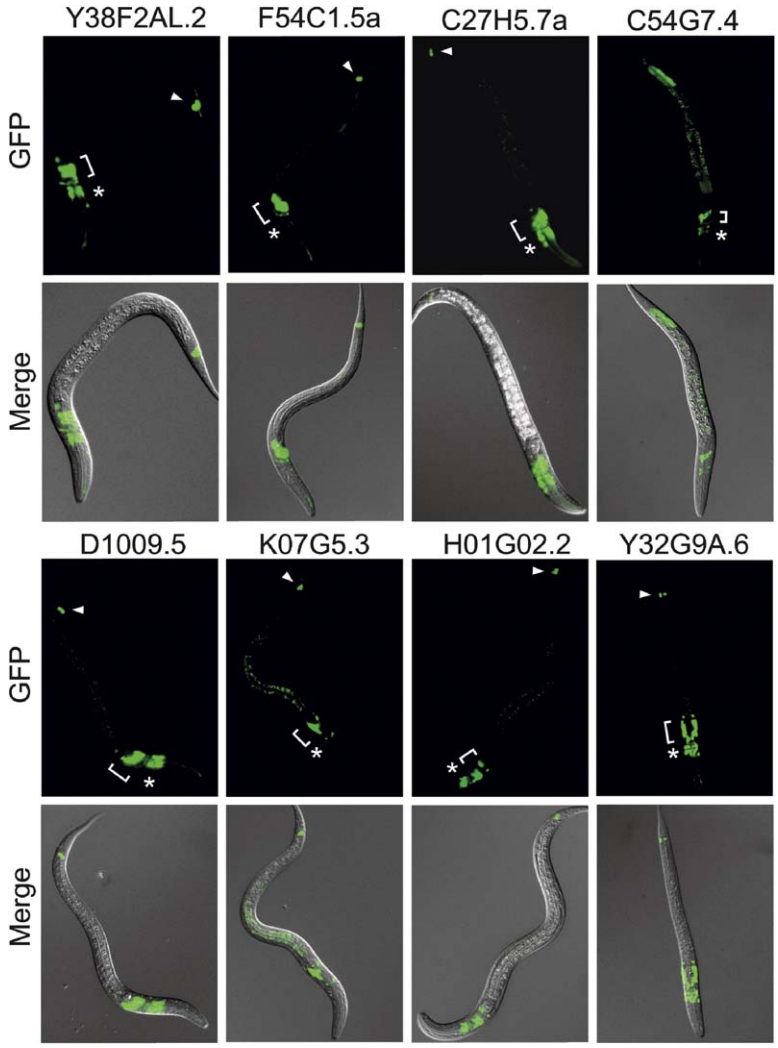


Figure 1. Expression Analysis of Candidate Cilia-Related Genes Identifies New Genes Expressed Exclusively in Ciliated Cells

Shown are whole-worm GFP and GFP/DIC merged images of transgenic animals expressing the indicated transcriptional *gfp* reporter. Expression is restricted to ciliated cells such as the amphid neurons (bracket), the labial-quadrant neurons (asterisk), and the phasmid-tail neurons (arrowhead). Note that for some markers (e.g., C54G7.4 and K07G5.3), the weak signals along the midbody are due to the nonspecific autofluorescence of gut granules.

ponents. First described in *Chlamydomonas* [15], IFT involves the kinesin- and dynein-dependent bidirectional movement of IFT particles and associated cargo along ciliary axonemes [1–3, 15]. In *C. elegans*, anterograde transport of IFT particles along the middle segment of cilia is driven cooperatively by two Kinesin-2 motors (heterotrimeric Kinesin-2 and homodimeric OSM-3) and by OSM-3 alone along the distal segments [16]. IFT particles have been shown biochemically to be composed of two large protein complexes (A and B) containing at least 16 proteins in total [17, 18].

Using time-lapse microscopy, we examined animals expressing C27H5.7a::*gfp* and found that the GFP-tagged protein exhibited IFT along ciliary axonemes of head and tail neurons (Figure S4B; Document S2; Movies S1 and S4). Anterograde transport rates along the middle and distal segments were determined to be 0.70 ± 0.11 μm/s (n = 245) and 1.25 ± 0.15 μm/s (n = 255), respectively, with the retrograde transport rate estimated to be 1.32 ± 0.2 μm/s (n = 5). Remarkably, these transport rates for C27H5.7a::GFP are almost identical to those previously reported for the Kinesin-2 motors and IFT particle components [1, 16], indicating that C27H5.7a is transported with IFT particles by heterotrimeric Kinesin-2 and OSM-3 within the middle segments of ciliary axonemes and by OSM-3 kinesin alone within the distal segments.

We then examined the behavior of C27H5.7a::GFP in two IFT mutant strains, namely *osm-5(p813)* and *che-11(e1810)*, both of which possess truncated cilia and display abrogated IFT. In these mutants, C27H5.7a::GFP displayed little or no detectable IFT and accumulated in the dendrite and transition zones of the *osm-5* mutant, as well as within the transition zones and along the ciliary axonemes in the *che-11* background (Figure 2A; Document S2; Movies S2, S3, S5, and S6). The dependence of C27H5.7a on *osm-5* and *che-11* for its normal localization and motility strongly suggests that C27H5.7a is part of the motor-IFT particle-cargo complex. To provide further evidence that C27H5.7a is likely a core component (and not cargo) of IFT particles, we studied its behavior in *bbs* mutant backgrounds. Previously, we observed that GFP-tagged CHE-2 often accumulated near the midpoint and distal segments of ciliary axonemes in *bbs* mutants [19]. We now show that three other GFP-tagged IFT components, namely

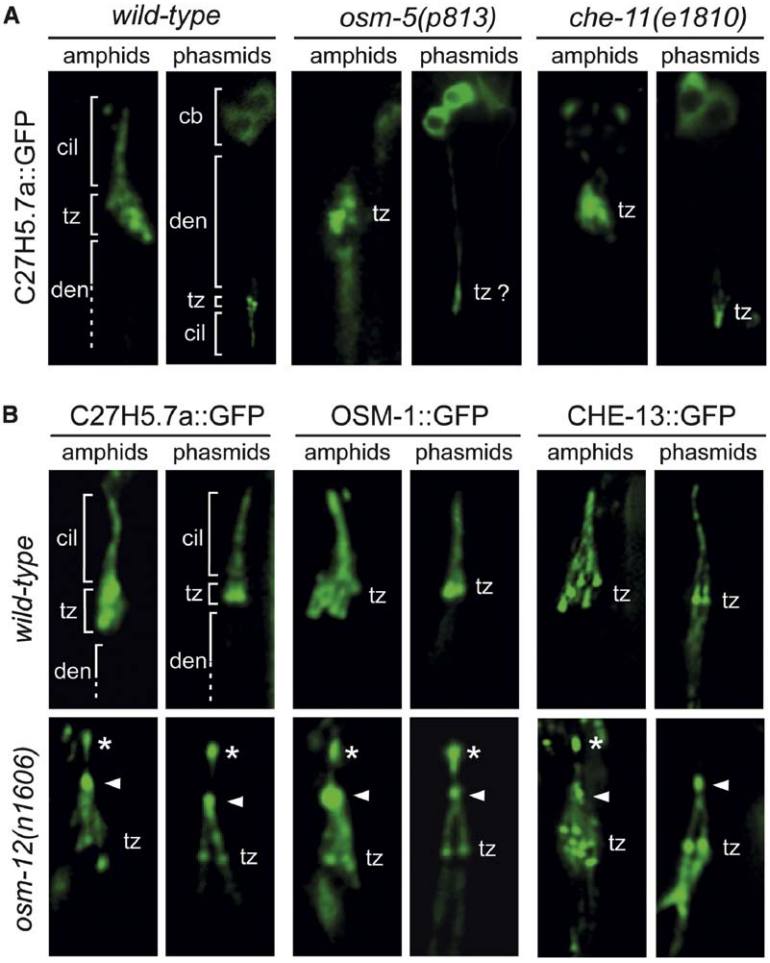


Figure 2. The Ciliary Localization of C27H5.7a Is Disrupted by Mutations in IFT and *bbs* Genes

Shown are one set of amphid and phasmid cilia, with the ciliary axonemes (cil), transition zones (tz), dendrites (den), and cell bodies (cb) indicated in the left-hand panels. All images are similarly sized and oriented, with the tz positions indicated in all panels.

(A) Localization of GFP-tagged C27H5.7a in wild-type, *osm-5(p813)*, and *che-11(e1810)* mutant backgrounds. In the wild-type, C27H5.7a::GFP localizes at the transition zones and along ciliary axonemes, whereas in *osm-5(p813)* and *che-11(e1810)* mutants, C27H5.7a::GFP accumulates at transition zones in *osm-5* mutants and along the stunted ciliary axonemes of *che-11* mutants. The question mark indicates that the tz position cannot be accurately identified.

(B) C27H5.7a::GFP mislocalizes along *bbs-7* (*osm-12(n1606)*) mutant cilia, displaying accumulation at the midpoint of the ciliary axonemes (arrowhead) and within the distal segment (asterisk). Similar mislocalization along *bbs-7* mutant cilia is also observed for four GFP-tagged IFT proteins, namely OSM-1, CHE-13, OSM-6, and CHE-2 (see Figure S5 for OSM-6::GFP and CHE-2::GFP images).

CHE-13, OSM-1, and OSM-6, demonstrate the same phenotype in a *bbs-7* mutant (*osm-12(n1606)*) (Figure 2B; data for CHE-2 and OSM-6 shown in Figure S5). Interestingly, when expressed in the *bbs-7* or *bbs-8* mutant backgrounds, C27H5.7a::GFP displays the same mislocalization phenotype as OSM-1, OSM-6, CHE-2, and CHE-13 (Figure 2B; Document S2; Movies S7–S16; data not shown for *bbs-8* mutant), suggesting

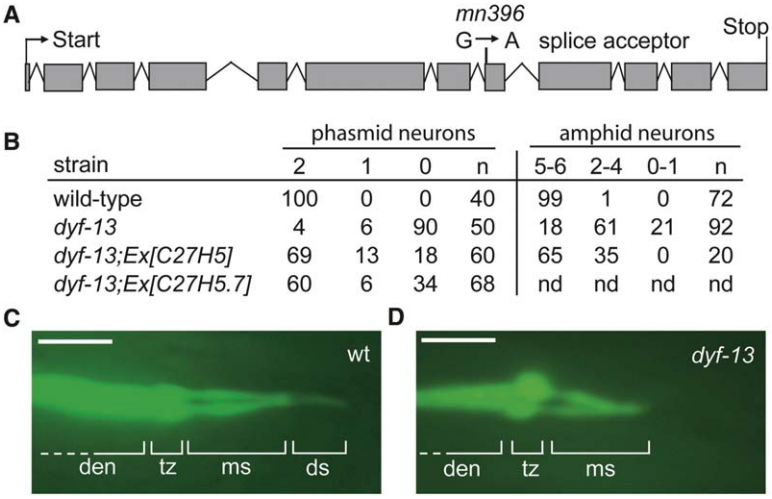


Figure 3. Mutation in C27H5.7a Causes the Structural Cilia Defect in *dyf-13(mn396)* Mutants

(A) A schematic of the putative exon/intron structure of C27H5.7a shows the guanine-to-adenine splice acceptor mutation in *dyf-13(mn396)*.

(B) The dye-uptake-defective phenotype (Dyf) of *dyf-13(mn396)* mutants is rescued by the C27H5 cosmid and by a transgene containing the wild-type C27H5.7a gene. Shown are the percentages of sensory organs with normal dye-fill in the indicated number of amphid and phasmid neurons. "n" denotes number of sensory organs scored and "nd" denotes not determined.

(C and D) The cilia of *dyf-13(mn396)* mutants are short, lacking distal portions. Shown are GFP images of animals expressing a *ceh-23* promoter*::gfp* transgene in the phasmid neurons. Anterior is to the left. Note that the phasmid cilia of *dyf-13* mutants are shorter than those of wild-type animals. The following abbreviations were used: den, dendrite; tz, transition zone; ms, middle segment; and ds, distal segment. The scale bar represents 5 μm.

that C27H5.7a is closely associated with IFT particle components and does not represent cargo.

### The *dyf-13* Mutant Contains a Mutation in C27H5.7a and Possesses Abnormal Cilia

To provide additional evidence that C27H5.7a is a core ciliary component, we searched existing sensory mutants for mutations in this gene. Using this approach, we found that *dyf-13(mn396)* animals contained a guanine-to-adenine mutation in the acceptor site of intron 7 of C27H5.7a (Figure 3A). *dyf-13* mutants are defective in sensory neuron dye filling and chemosensation [20]. Specifically, only 18% of amphid and 4% of phasmid sensory organs displayed wild-type dye filling (Figure 3B). This phenotype, comparable to that of IFT and *bbs* mutants [19–21], suggests that ciliary structures are compromised. Using a *ceh*-23 promoter*::gfp* reporter (gift of G. Garriga) that illuminates the cell bodies, dendrites, transition zones, and cilia of the phasmid neurons, we found that the cilia of *dyf-13* animals were indeed malformed (Figures 3C and 3D). Specifically, the average length of the cilium in *dyf-13*(*mn396*) animals was 6.7 ± 0.8 μm (n = 20) in comparison to 8.6 ± 1.6 μm (n = 20) in wild-type animals, and the neurons appeared to lack the distal portion of the cilia. This cilia defect is similar to that observed in animals harboring mutations in *osm-3*, an IFT-specific kinesin required to build the distal segment [16, 21]. Importantly, the dye-filling defect of *dyf-13(mn396)* mutants was similarly rescued in three independent lines expressing either the C27H5 cosmid or a transgene bearing the wild-type C27H5.7 gene (Figure 3B; data shown for one rescued line in each case).

On the whole, our findings provide strong evidence that DYF-13 (C27H5.7a) is an IFT protein that is important for the formation and function of cilia. Consistent with this conclusion, an uncharacterized human homolog (FLJ12571) with 37% amino acid identity and 59% similarity throughout its length exists, and counterparts are found in all ciliated organisms (including *Chlamydomonas reinhardtii*), but not in nonciliated organisms such as *Arabidopsis thaliana* or *Saccharomyces cerevisiae*.

### Supplemental Data

Detailed Experimental Procedures and several supplemental figures, movies, and tables are available at http://www.current-biology.com/cgi/content/full/15/10/935/DC1/.

### Acknowledgments

This work was funded by the Heart and Stroke Foundation of British Columbia and Yukon and the Canadian Institutes for Health Research (CIHR; CBM134736) (M.R.L.), the Patterson Trust and National Institutes of Health Medical Scientist Training Program (MSTP) grant GM07739 (S.S. and E.P.), Genome British Columbia and Genome Canada (D.G.M., D.L.B., M.A.M., and S.J.J.), and the Swedish Foundation for Strategic Research (SSF) (P.S.). M.R.L. acknowledges scholar awards from the CIHR and the Michael Smith Foundation for Health Research (MSFHR). D.L.B. holds a Canada Research Chair. O.E.B. acknowledges fellowships from the CIHR and the MSFHR. The work by G.O. was supported by a grant (NIH GM 50718) to Jonathan M. Scholey. We thank Kenta Asahina for sequencing of the *dyf-13(mn396)* allele. Correspondence relating to *dyf-13(mn396)* (phenotypic characterization and cloning of the mutation) should be addressed to S.S.

Received: January 3, 2005
Revised: April 13, 2005
Accepted: April 18, 2005
Published: May 24, 2005

### References

1. Scholey, J.M. (2003). Intraflagellar transport. Annu. Rev. Cell Dev. Biol. *19*, 423–443.
2. Rosenbaum, J.L., and Witman, G.B. (2002). Intraflagellar transport. Nat. Rev. Mol. Cell Biol. *3*, 813–825.
3. Pazour, G.J., and Rosenbaum, J.L. (2002). Intraflagellar transport and cilia-dependent diseases. Trends Cell Biol. *12*, 551–555.
4. Katsanis, N., Lupski, J.R., and Beales, P.L. (2001). Exploring the molecular basis of Bardet-Biedl syndrome. Hum. Mol. Genet. *10*, 2293–2299.
5. Ansley, S.J., Badano, J.L., Blacque, O.E., Hill, J., Hoskins, B.E., Leitch, C.C., Kim, J.C., Ross, A.J., Eichers, E.R., Teslovich, T.M., et al. (2003). Basal body dysfunction is a likely cause of pleiotropic Bardet-Biedl syndrome. Nature *425*, 628–633.
6. Swoboda, P., Adler, H.T., and Thomas, J.H. (2000). The RFX-type transcription factor DAF-19 regulates sensory neuron cilium formation in *C. elegans*. Mol. Cell *5*, 411–421.
7. Saha, S., Sparks, A.B., Rago, C., Akmaev, V., Wang, C.J., Vogelstein, B., Kinzler, K.W., and Velculescu, V.E. (2002). Using the transcriptome to annotate the genome. Nat. Biotechnol. *20*, 508–512.
8. McKay, S.J., Johnsen, R., Khattra, J., Asano, J., Baillie, D.L., Chan, S., Dube, N., Fang, L., Goszczynski, B., Ha, E., et al. (2003). Gene expression profiling of cells, tissues, and developmental stages of the nematode *C. elegans*. Cold Spring Harb. Symp. Quant. Biol. *68*, 159–169.
9. Fan, Y., Esmail, M.A., Ansley, S.J., Blacque, O.E., Boroevich, K., Ross, A.J., Moore, S.J., Badano, J.L., May-Simera, H., Compton, D.S., et al. (2004). Mutations in a member of the Ras superfamily of small GTP-binding proteins causes Bardet-Biedl syndrome. Nat. Genet. *36*, 989–993.
10. Li, J.B., Gerdes, J.M., Haycraft, C.J., Fan, Y., Teslovich, T.M., May-Simera, H., Li, H., Blacque, O.E., Li, L., Leitch, C.C., et al. (2004). Comparative genomics identifies a flagellar and basal body proteome that includes the BBS5 human disease gene. Cell *117*, 541–552.
11. Otto, E.A., Schermer, B., Obara, T., O'Toole, J.F., Hiller, K.S., Mueller, A.M., Ruf, R.G., Hoefele, J., Beekmann, F., Landau, D., et al. (2003). Mutations in INVS encoding inversin cause nephronophthisis type *2*, linking renal cystic disease to the function of primary cilia and left-right axis determination. Nat. Genet. *34*, 413–420.
12. Avidor-Reiss, T., Maer, A.M., Koundakjian, E., Polyanovsky, A., Keil, T., Subramaniam, S., and Zuker, C.S. (2004). Decoding cilia function: Defining specialized genes required for compartmentalized cilia biogenesis. Cell *117*, 527–539.
13. Ostrowski, L.E., Blackburn, K., Radde, K.M., Moyer, M.B., Schlatzer, D.M., Moseley, A., and Boucher, R.C. (2002). A proteomic analysis of human cilia: Identification of novel components. Mol. Cell. Proteomics *1*, 451–465.
14. Colosimo, M.E., Brown, A., Mukhopadhyay, S., Gabel, C., Lanjuin, A.E., Samuel, A.D., and Sengupta, P. (2004). Identification of thermosensory and olfactory neuron-specific genes via expression profiling of single neuron types. Curr. Biol. *14*, 2245–2251.
15. Kozminski, K.G., Johnson, K.A., Forscher, P., and Rosenbaum, J.L. (1993). A motility in the eukaryotic flagellum unrelated to flagellar beating. Proc. Natl. Acad. Sci. USA *90*, 5519–5523.
16. Snow, J.J., Ou, G., Gunnarson, A.L., Walker, M.R., Zhou, H.M., Brust-Mascher, I., and Scholey, J.M. (2004). Two anterograde intraflagellar transport motors cooperate to build sensory cilia on *C. elegans* neurons. Nat. Cell Biol. *6*, 1109–1113.
17. Piperno, G., and Mead, K. (1997). Transport of a novel complex

in the cytoplasmic matrix of *Chlamydomonas* flagella. Proc. Natl. Acad. Sci. USA *94*, 4457–4462.

18. Cole, D.G., Diener, D.R., Himelblau, A.L., Beech, P.L., Fuster, J.C., and Rosenbaum, J.L. (1998). *Chlamydomonas* kinesin-II-dependent intraflagellar transport (IFT): IFT particles contain proteins required for ciliary assembly in *Caenorhabditis elegans* sensory neurons. J. Cell Biol. *141*, 993–1008.
19. Blacque, O.E., Reardon, M.J., Li, C., McCarthy, J., Mahjoub, M.R., Ansley, S.J., Badano, J.L., Mah, A.K., Beales, P.L., Davidson, W.S., et al. (2004). Loss of *C. elegans* BBS-7 and BBS-8 protein function results in cilia defects and compromised intraflagellar transport. Genes Dev. *18*, 1630–1642.
20. Starich, T.A., Herman, R.K., Kari, C.K., Yeh, W.H., Schackwitz, W.S., Schuyler, M.W., Collet, J., Thomas, J.H., and Riddle, D.L. (1995). Mutations affecting the chemosensory neurons of *Caenorhabditis elegans*. Genetics *139*, 171–188.
21. Perkins, L.A., Hedgecock, E.M., Thomson, J.N., and Culotti, J.G. (1986). Mutant sensory cilia in the nematode *Caenorhabditis elegans*. Dev. Biol. *117*, 456–487.